Hindawi
Shock and Vibration
Volume 2017, Article ID 7285216, 10 pages
https://doi.org/10.1155/2017/7285216

Research Article

The Absolute Deviation Rank Diagnostic Approach to Gear Tooth Composite Fault

Guangbin Wang, Wenhui Deng, Xiaoyang Du, and Xuejun Li

Hunan Provincial Key Laboratory of Health Maintenance for Mechanical Equipment, Hunan University of Science & Technology, Xiangtan 411210, China

Correspondence should be addressed to Guangbin Wang; jxxwgb@126.com

Received 17 October 2016; Accepted 7 December 2016; Published 9 January 2017

Academic Editor: Luca Collini

Aiming at nonlinear and nonstationary characteristics of the different degree with single fault gear tooth broken, pitting, and composite fault gear tooth broken-pitting, a method for the diagnosis of absolute deviation of gear faults is presented. The method uses ADAMS, respectively, set-up dynamics model of single fault gear tooth broken, pitting, and composite fault gear tooth broken-pitting, to obtain the result of different degree of broken teeth, pitting the single fault and compound faults in the meshing frequency, and the amplitude frequency doubling through simulating analysis. Through the comparison with the normal state to obtain the sensitive characteristic of the fault, the absolute value deviation diagnostic approach is used to identify the fault and validate it through experiments. The results show that absolute deviation rank diagnostic approach can realize the recognition of gear single faults and compound faults with different degrees and provide quick reference to determine the degree of gear fault.

1. Introduction

Gearbox, as one of the core parts of mechanical transmission system, is extremely prone to various faults due to the long run under harsh working environment. As a matter of fact, the fault does not often appear alone; the gear failures of broken teeth and pitting usually easily lead to broken teeth-pitting composite failures [1–4]. In recent years, many scholars are dedicated to extraction and recognition research of gear fault feature, and it has made a great achievement. Kar and Mohanty [5] use multiresolution Fourier transform to diagnose the gearbox under different load. Lei and Tang [6] set up planetary gearbox vibration signal simulation model based on analysis of the transmission mechanism to obtain different gear fault vibration response signal and compared it with the different normal and fault signal features in order to recognize the planetary gearbox failures. Chen and Yu [7], respectively, make analysis to the envelope order harmonic components and impact components, based on morphological differences of component and the measured speed signal between rolling bearings and gears contained in wind turbine gearbox composite failure vibration signals and its effectively separated gears fault feature under variable speeds from rolling bear. Zhan et al. [8] used the autoregressive model to analyze the residual signal of the gears containing the impact components. It was proved that the order of the AR model was correlated with the load. By satisfying the response statistic based on the AR model error signal, an AR model suitable for the diagnosis of variable load gear condition can be obtained.

The paper puts forward the absolute deviation rank diagnostic approach to broken teeth-pitting composite fault, and it took single broken teeth fault, pitting, and composite broken teeth-pitting fault as the research object, using ADAMS to establish gear teeth broken-pitting compound fault dynamics model and single failure dynamic model. It obtained the single fault and multifault frequency value in the meshing frequency and multiple frequency after the Fourier transformation to simulation data. The absolute value deviation diagnostic approach is proposed based on the normal state of the meshing frequency and the absolute value of frequency multiplication, and the frequency multiplication of different degrees and different types of faults is obtained. The fault sensitive features are determined and verified by experiments.

2. Based on ADAMS Dynamic Model of Gear Tooth Broken-Pitting

It is a key point to calculate the meshing stiffness of gears when it builds dynamic model of gear transmission system in ADAMS [9]. Many scholars have a deep research [10] and they all considered that it can effectively simulate the gear bending and torsional deformation through adding auxiliary gear and torsional spring [11–14].

Assuming that the gear drive is described by n generalized coordinates q, after introducing the contact constraint condition, its dynamic equation is expressed as [15]

$$\begin{aligned} M\ddot{q} + Kq + \lambda\phi_q^T &= Q + F \\ \phi(q,t) &= 0, \end{aligned} \tag{1}$$

where M and K are the generalized mass matrix and the generalized stiffness matrix; ϕ is the constraint equation; ϕ_q is the Jacobian matrix of the constraint equation; λ is the Lagrange multiplier; Q is the generalized force matrix; and F is the contact force.

According to the contact mechanics theory, the contact force is reduced to the equivalent spring-damping model. The generalized expression is

$$F = K\delta^n + C(\delta)\dot{\delta}, \tag{2}$$

where K is the equivalent contact stiffness of meshing tooth profile elasticity; δ is the deformation of the meshing point; n is a nonlinear elasticity exponent and $n \geq 1$; $C(\delta)$ is a deformation-based contact damping polynomial that describes the energy loss during gear meshing; $\dot{\delta}$ is the tooth profile deformation speed.

The moment of inertia and the effective area of contact will change, resulting in a change in stiffness while the gears are in motion. Therefore, calculate the equivalent stiffness values of the gears under different faults, and input ADAM to achieve the simulation analysis. The equivalent stiffness of the gear meshing is calculated as [16]

$$K = \frac{1}{k_h} + \frac{1}{k_b} + \frac{1}{k_a} + \frac{1}{k_s} + \frac{1}{k_f}, \tag{3}$$

where k_h is the failure of the Hertz stiffness; k_b is bending stiffness; k_a is radial stiffness, k_s is shear stiffness; k_f is tooth base stiffness.

The meshing Hertz stiffness of the same material is

$$k_h = \frac{\pi EL}{4(1-\nu^2)}, \tag{4}$$

where E is the elastic potential energy, L is the axial thickness of the gear, and ν is Poisson's ratio.

Tooth base stiffness k_f is

$$\begin{aligned} \frac{1}{k_f} = \frac{\cos^2\alpha}{EL}\left\{L^*\left(\frac{u_f}{s_f}\right)^2 + M^*\left(\frac{u_f}{s_f}\right)\right. \\ \left. + P^*\left(1 + Q^*\tan^2\alpha\right)\right\}, \end{aligned} \tag{5}$$

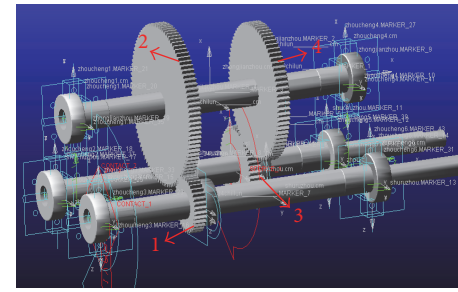

Figure 1: Dynamic model of gear transmission system.

where X^* represents the coefficients L^*, M^*, P^*, and Q^*. $h_f = r_f/r$, and r_f is the root diameter. The remaining parameters are described in [10].

The bending stiffness and shear stiffness are

$$\begin{aligned} \frac{1}{k_b} &= \int_{-a_1}^{a_2} \frac{\{1 + \cos\alpha_1\left[(\alpha_2 - \alpha)\sin\alpha - \cos\alpha\right]\}^2 (\alpha_2 - \alpha_1)\cos\alpha}{2EI_{xc}} d\alpha \\ \frac{1}{k_s} &= \int_{-a_1}^{a_2} \frac{1.2(1+\nu)(\alpha_2 - \alpha)\cos\alpha\cos^2\alpha_1}{2EA_{xc}} d\alpha, \end{aligned} \tag{6}$$

where L is the axial thickness of the gear; ν is Poisson's ratio; R_{b1} is the base circle radius of the pinion. α_2 is the pressure angle of the faulty contact point; α is the pressure angle.

I_{xc} and A_{xc} are the effective moment of inertia and the cross-sectional area distance from the tooth root x, respectively, when the gear is faulted.

$$\begin{aligned} I_{xc} &= \frac{1}{12} \\ &\quad \cdot R_{b1}\left\{\left[\sin\alpha_2 + (\alpha_2 + \alpha)\cos\alpha - \sin\alpha\right] - q\sin\nu\right\}^3 L \\ A_{xc} &= \left\{R_{b1}\left[\sin\alpha_2 + (\alpha_2 - \alpha)\cos\alpha - \sin\alpha\right] - q\sin\nu\right\} \\ &\quad \cdot L. \end{aligned} \tag{7}$$

As shown in Figure 1, the dynamic model of gear transmission system was built with normal state in ADAMS [17].

The gear transmission system was designed for double-stage driving. It concludes three shafts which contain input shaft, intermediate shaft, output shaft, and two pairs of gears where gear 1 meshed with 2 and gear 3 meshed with 4.

It will generate gear bending, torsional, and contact deformation in the mesh movement, and the contact deformation of the tooth surface can cause the change of meshing stiffness and damping. Then, based on the dynamic model of the gear transmission system in Figure 1, the fault geometry is implanted in the solid model of the gear transmission system, which can effectively simulate the dynamic effects of gear tooth breakage and pitting failure through the contact algorithm in ADAMS software. It established dynamics model of single fault to broken teeth, pitting, and broken teeth-pitting composite fault through changing the geometry in the three-dimensional entity model. Specifically, as shown in

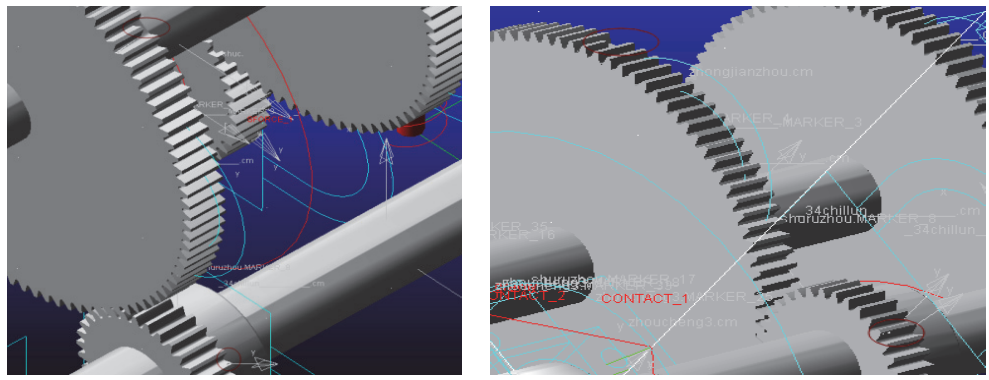

(a) Composite fault 1 kinetic model

(b) Composite fault 2 kinetic model

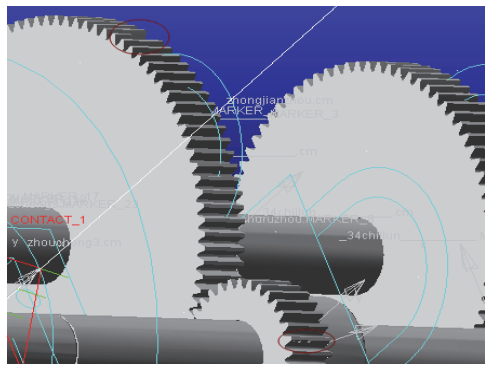

(c) Composite fault 3 kinetic model

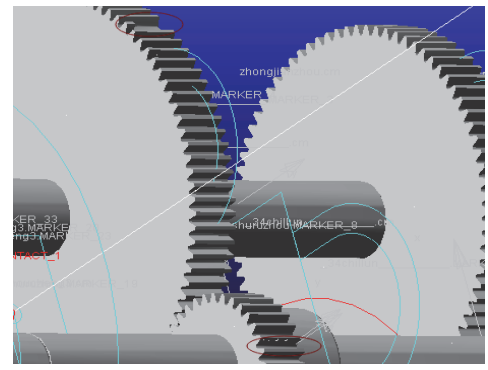

(d) Composite fault 4 kinetic model

Figure 2: Dynamics model of the gear broken teeth-pitting compound fault.

Figure 2, four different degrees of broken gear failure include 1/5 broken teeth, 2/5 broken teeth, 3/5 broken teeth, and 4/5 broken teeth; four different kinds of gear pitting failure include pitting 1 which is to form a circle with a diameter of 4 mm, pitting 2 which is based on pitting 1 to form a diameter of 5 mm circle, pitting 3 which is based on pitting 2 more than a diameter of 6 mm circle, and pitting 4 which is in pitting 3 on the basis of more than a diameter of 7 mm circle. The composite fault is obtained by combining the broken tooth with the pitting failure, composite failure 1 is the combination of the broken tooth 1 and the pitting corrosion 1, and then the compound fault of different degrees can be obtained by analogy.

3. The Time-Frequency Statistics Analysis of Gear Failure

There are four different degrees of broken teeth-pitting compound fault simulated with three kinds of load and three types of speed, where the load in size is 0 N·m, 975 N·m, and 1790 N·m and the motor in speed is 10 Hz, 20 Hz, and 30 Hz. The statistical analysis includes the peak-peak value and the root-mean-square value, in which the peak-peak value is defined as the difference between the single peak maximum value and the single peak minimum value and is positive. The root mean square (RMS) value is named as the effective value representing the energy of vibration signal, and it is an important index to judge whether the machine running state is normal or not in mechanical fault diagnosis, and the statistical results are shown in Figures 3~6.

Comparing four different degrees of composite fault analysis data with speed peak-peak value, we can see from Figures 3–6 that the vibration signal amplitude value increased with the degree of gear composite fault and the speed of values becomes more obvious as the growing of load during the speed from 600 RPM to 1800 RPM; the trend is upward as a whole. The skewness about vibration signal significantly increased when speed crosses around 1200 RPM; that is to say, the vibration of gear system increased along with the deepening of fault degree. Since the RMS reflects the energy change, we can know that the larger RMS value, the greater energy of the system and the greater the impact vibration of gears system.

According to Figure 7, the peak-peak value of the compound fault increased with the augment of the rotating speed under the same load 1790 N·m, and the amplitude value increased with the augment of the fault degree. The RMS value of the composite fault in different degree increased with the augment of the rotational speed, and the RMS value of the amplitude changes little in different complex failure when it works in rotating speed 600~1200 RPM. The RMS value increases with the augment of the rotational speed when the rotating speed is 1200~1800 RPM, which indicates the greater

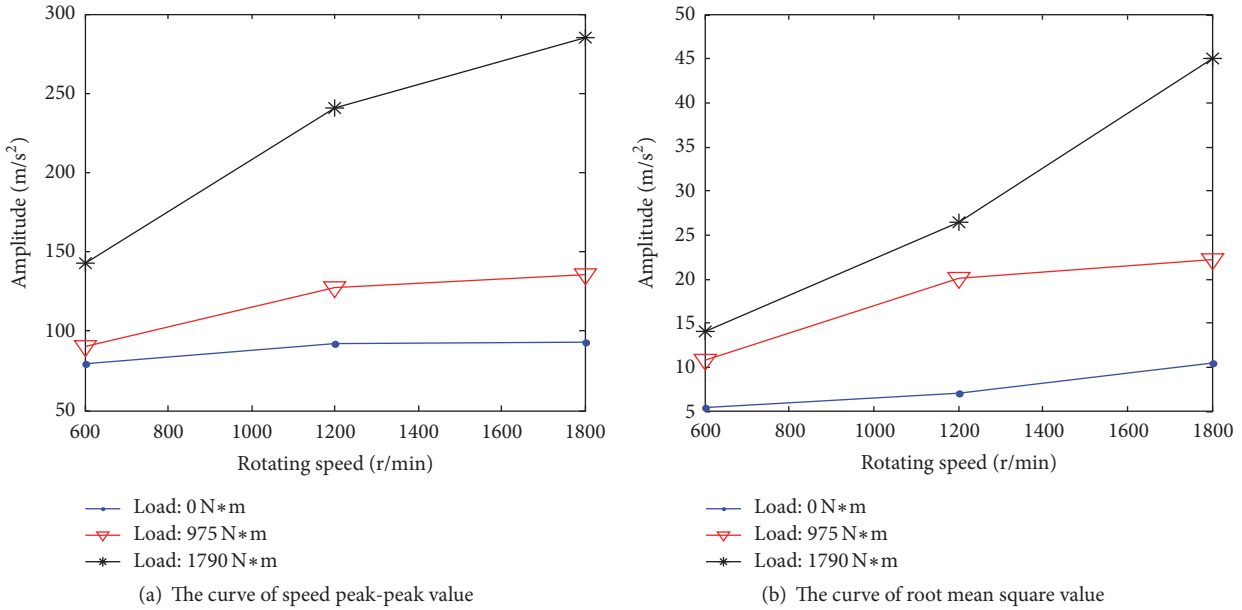

(a) The curve of speed peak-peak value (b) The curve of root mean square value

Figure 3: Broken teeth-pitting compound fault 1.

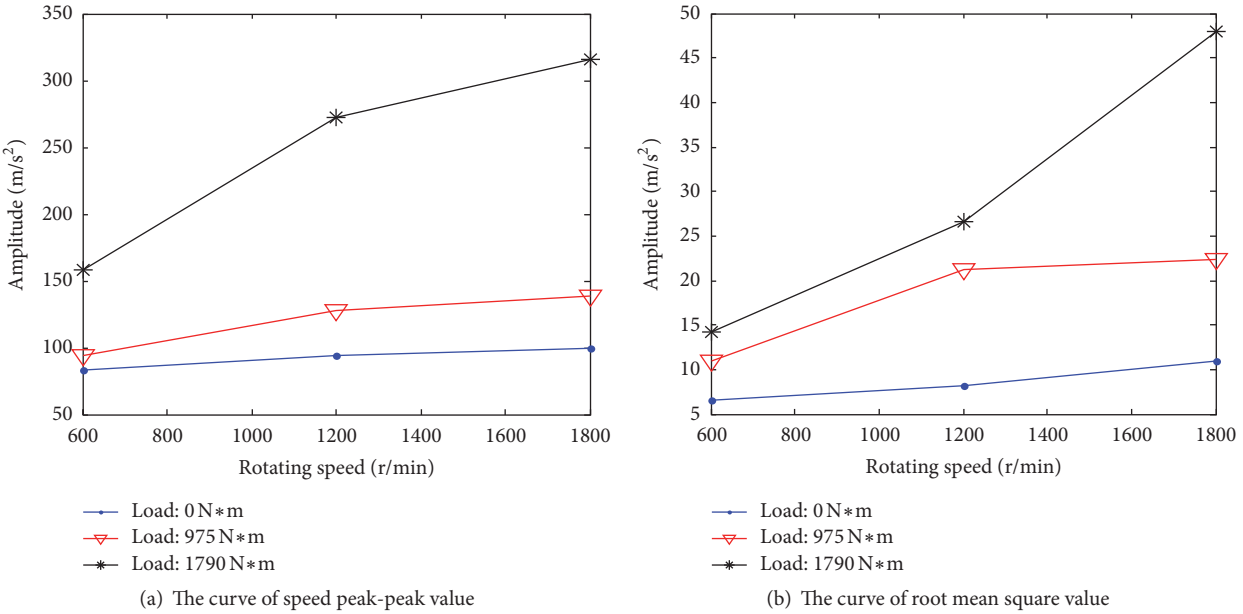

(a) The curve of speed peak-peak value (b) The curve of root mean square value

Figure 4: Broken teeth-pitting compound fault 2.

vibration impact of the gear system with the expanding fault degree and increasing speed.

From the analysis above, we can know the greater impact strength while the gear is meshing, and it followed with the growth of the rotating speed when it is under the same degree of broken teeth composite fault and speed; the bigger load, the greater impact strength in gear mesh when it is under the same degree of broken teeth and load; the greater load leads to worse broken teeth composite fault and greater impact strength in the gear mesh when it is under the same rotating speed and load.

4. Based on Gear Tooth Broken-Point Erosion Composite Fault of the Absolute Deviation Rank Diagnostic Approach

Based on simulation results, the frequency domain graph about gear teeth broken, gear pitting single failure, and broken teeth-pitting composite failures is obtained. The fault characteristics can be observed directly from the simulation curve, and the type of fault can be easily identified under the condition of known fault type and fault degree, since the original signal obtained from spot test includes racket

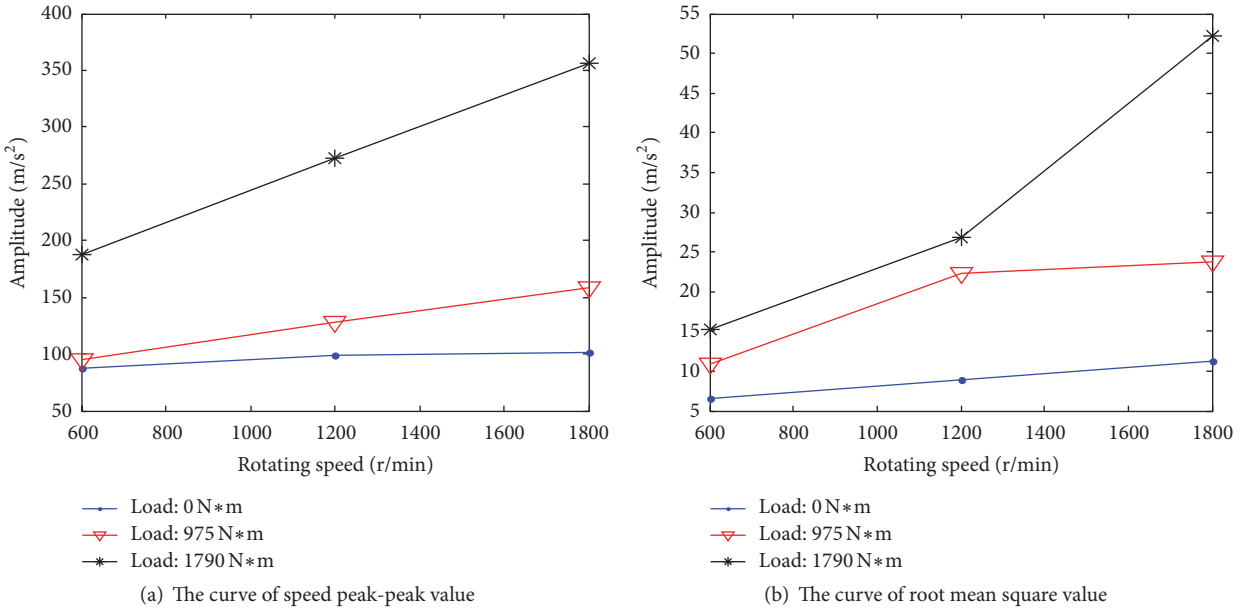

(a) The curve of speed peak-peak value

(b) The curve of root mean square value

Figure 5: Broken teeth-pitting compound fault 3.

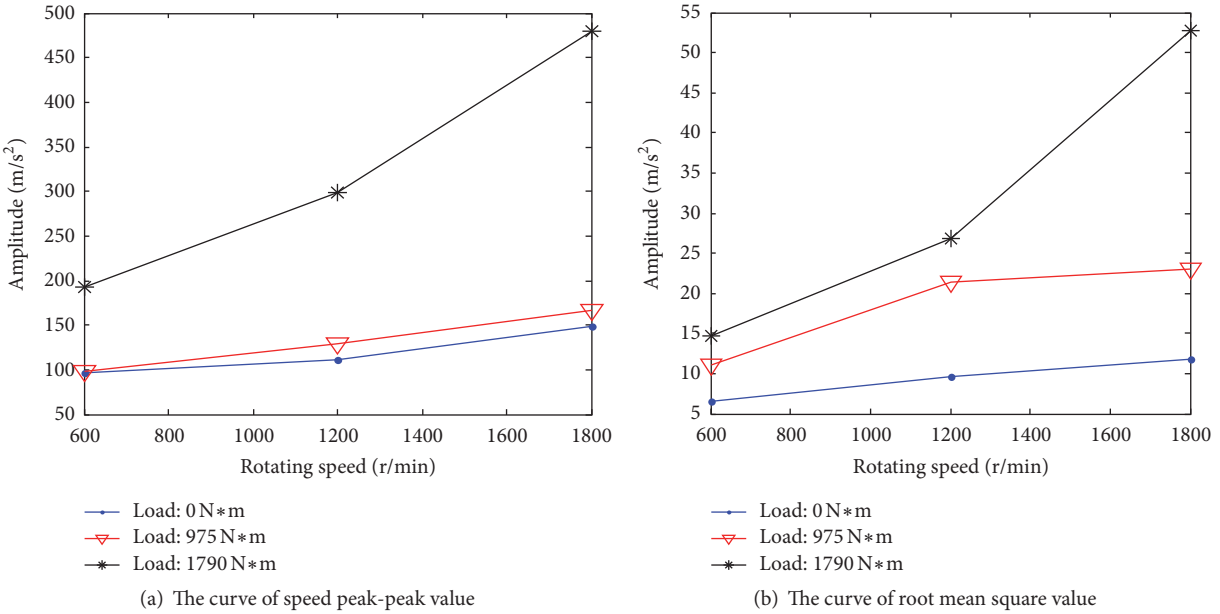

(a) The curve of speed peak-peak value

(b) The curve of root mean square value

Figure 6: Broken teeth-pitting compound fault 4.

interference signal and it is hard to identify its fault type and degree and to found out its characteristic rules from the time-frequency diagram.

Therefore, the data is comprehensively analyzed based on the simulation results. Firstly, according to the type of fault and the degree of failure to classify, with the numbers 1 to 14, the specific situation is shown in Table 1.

Secondly, in order to realize the identification and monitoring of fault types, as shown in Table 2, the obtained simulation results are classified according to the tooth broken, pitting, and tooth broken-pitting corrosion.

According to the result of Table 2, it assumes a normal model as a benchmark on the basis of gear failure simulation, selecting vibration amplitude of sensitive feature, and the corresponding feature frequency as the identification of the fault parameters. Each of the simulated fault characteristic frequency amplitudes is compared with normal amplitude and takes it as an absolute deviation calculation; the results are shown in Table 3.

The absolute deviation formula is

$$\left|\Delta_i\right| = \frac{\left(a_i - a_i^n\right)}{a_i^n} \times 100\%, \tag{8}$$

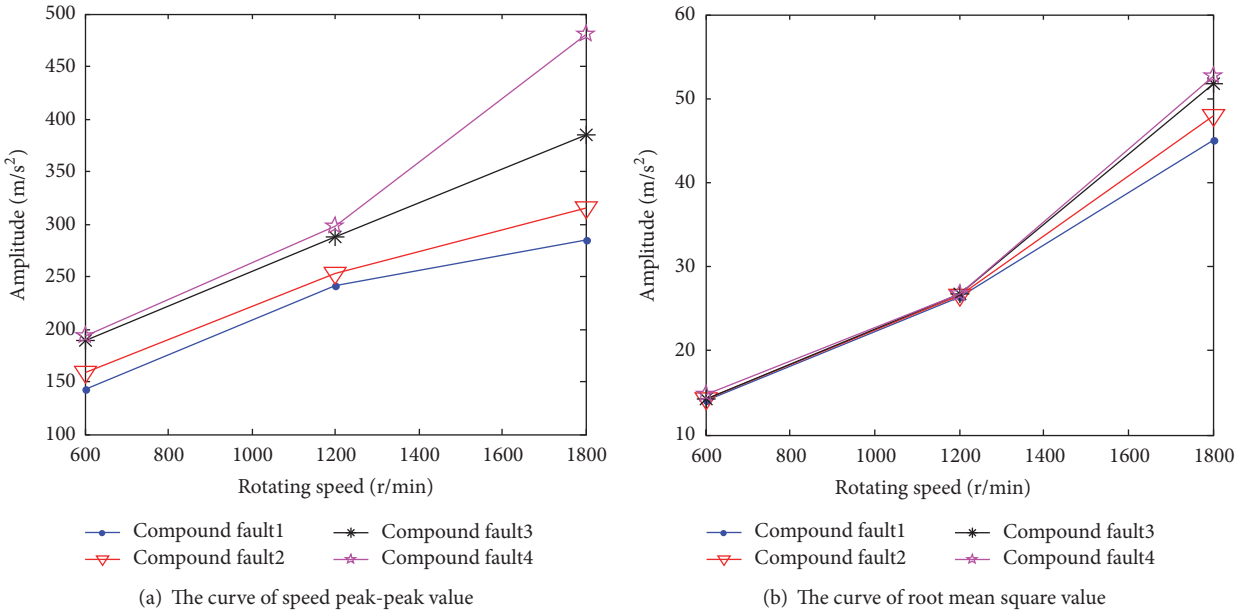

(a) The curve of speed peak-peak value

(b) The curve of root mean square value

Figure 7: The curve of compound fault on load 1790 N·m.

Table 1: The code of simulation faults model.

Number	Fault type	Fault degree
1	Normal model	Nonfault
2	1/5 broken teeth	Seriousness
3	2/5 broken teeth	Seriousness
4	3/5 broken teeth	Seriousness
5	4/5 broken teeth	Seriousness
6	Total broken teeth	Seriousness
7	Point erosion 1	Slight
8	Point erosion 2	General
9	Point erosion 3	Seriousness
10	Point erosion 4	Seriousness
11	Compound fault 1	General
12	Compound fault 2	Seriousness
13	Compound fault 3	Seriousness
14	Compound fault 4	Seriousness

where a_i $(i = 1, 2, 3, 4, 5)$ represents the vibration signal of the fault model in mesh and multiple frequency amplitude and a_i^n is the responding frequency amplitude of the normal model.

In order to quickly extract the fault features from three different fault types, it is more intuitive to judge the fault type of the gears in the actual operation so as to achieve the purpose of fault recognition. After we got the calculation results of absolute deviation and divided the absolute deviation into several grades, where setting the absolute deviation as less than 1 as grade 0, setting the absolute deviation within the range of 1~4 as grade I, setting the absolute deviation within the range of 4~7 as grade II, setting the absolute deviation within the range of 7~10 as grade III, setting the absolute deviation within the range of 10~13 as grade IV, and setting the absolute deviation over 13 as grade V, then Table 3 can be rewritten as Table 4.

Table 4 is the results of the broken teeth, pitting, and broken teeth-pitting compound fault compared with normal model after classification and treatment, in order to more intuitively analyze each of absolute deviation rank values differences to identify the type of fault. Table 4 can be changed as pillars diagram, setting the absolute deviation rank 0 as 1 and setting the absolute deviation rank I as 2, and the rest is analogized in sequence, so Table 4 can be changed as in Figure 8.

We can see from Figure 8 and Table 4 that the absolute deviation of each fault type in the amplitude of the characteristic frequency is different. We can calculate its absolute deviation to identify the fault for the broken teeth because of little change in meshing frequency amplitude; there exists I rank deviation in second-time frequency amplitude and the same applies to the one-time frequency amplitude, which suggests that the feature frequency amplitude is sensitive fault parameters of broken teeth. There are three I rank deviations and one II rank deviation in the first-three-time frequency, which indicate that it is the point erosion fault sensitive parameters. There are three II rank deviations and one II rank deviation in double frequency amplitude, which are fault sensitive parameters for broken teeth-point erosion compound fault.

From Figure 8 and Table 4 absolute deviation level can be drawn to a fault and its different degree of sensitivity of the characteristic frequency can be analyzed by the corresponding characteristic frequency amplitude changes in the absolute deviation of the table to determine whether the level of the existence is of a gear failure.

Table 2: The fault simulation data.

Number	Fault type	Different fault of vibration amplitude in mesh frequency and multiple frequency				
		286 Hz	572 Hz	858 Hz	1144 Hz	1430 Hz
1	Normal model	23310	70770	40960	11970	9438
2	1/5 broken teeth	23190	72690	41260	12340	9021
3	2/5 broken teeth	23180	72050	41220	12200	9231
4	3/5 broken teeth	23150	71950	41220	12550	9040
5	4/5 broken teeth	23130	72120	41790	12850	9094
6	Total broken teeth	23300	68380	39720	12530	9305
7	Point erosion 1	22050	67400	38990	11210	8328
8	Point erosion 2	22630	79110	40410	9656	10040
9	Point erosion 3	22530	80410	40900	10090	9653
10	Point erosion 4	22550	81120	40890	10310	9856
11	Compound fault 1	23570	73470	41260	11890	9329
12	Compound fault 2	22280	67420	37130	9816	8892
13	Compound fault 3	21930	61100	39320	10510	9356
14	Compound fault 4	22020	70210	37660	10500	8163

Table 3: The absolute deviation of different fault types vibration frequency amplitude.

Number	Fault type	Different fault of absolute deviation in mesh frequency and multiple frequency (100%)				
		$\lvert\Delta_1\rvert$	$\lvert\Delta_2\rvert$	$\lvert\Delta_3\rvert$	$\lvert\Delta_4\rvert$	$\lvert\Delta_5\rvert$
1	Normal model	0	0	0	0	0
2	1/5 broken teeth	0.51	2.71	0.73	3.09	4.42
3	2/5 broken teeth	0.56	1.81	0.63	1.92	2.19
4	3/5 broken teeth	0.69	1.67	0.63	4.85	4.22
5	4/5 broken teeth	0.77	1.91	2.03	7.35	3.64
6	Total broken teeth	0.04	3.38	+	4.68	1.43
7	Point erosion 1	5.41	4.76	4.81	6.35	11.76
8	Point erosion 2	2.92	11.78	1.34	19.33	6.38
9	Point erosion 3	3.35	13.62	0.15	15.71	2.28
10	Point erosion 4	3.26	14.62	0.17	13.87	4.43
11	Compound fault 1	1.12	3.82	0.73	0.67	1.15
12	Compound fault 2	4.42	4.73	9.35	17.99	6.14
13	Compound fault 3	5.92	13.66	4.00	12.20	0.87
14	Compound fault 4	5.53	0.79	8.06	12.28	13.51

5. Experimental Verification

It takes fault simulation test bench of the American Quest Spectra company as object, and the vibration signal was collected by PULSE acquisition system. The end of the gearbox output axle connected to the brake, which changes the braking torque by adjusting the current with the electromagnetic brake and the sensor layout as shown in Figure 9.

Setting experimental conditions, the speed of the motor respectively is 10 Hz, 20 Hz, and 30 Hz, the current electromagnetic brake is set to 55 mA, where the brake torque is 1790 N·m, and sampling frequency of acquisition system is 16384 Hz, the acquisition time is 10 s, and pulley transmission ratio is 1 : 3.56.

Four different degrees of broken teeth, pitting single fault, and broken teeth-pitting composite failure are obtained by PULSE acquisition system. The vibration signals of different degrees of fault are obtained by experiment, the frequency amplitude in meshing frequency, and multiple frequency place to be obtained after engaging Fourier transform and the results are shown in Table 5.

The calculation was carried out with absolute deviation for the experimental data, and the obtained results are divided into several levels, where setting the absolute deviation as less than 1 as grade 0, setting the absolute deviation within the range of 1 to 4 as grade I, setting the absolute deviation within the range of 4 to7 as grade II, setting the absolute deviation within the range of 7~10 as grade III, setting the absolute

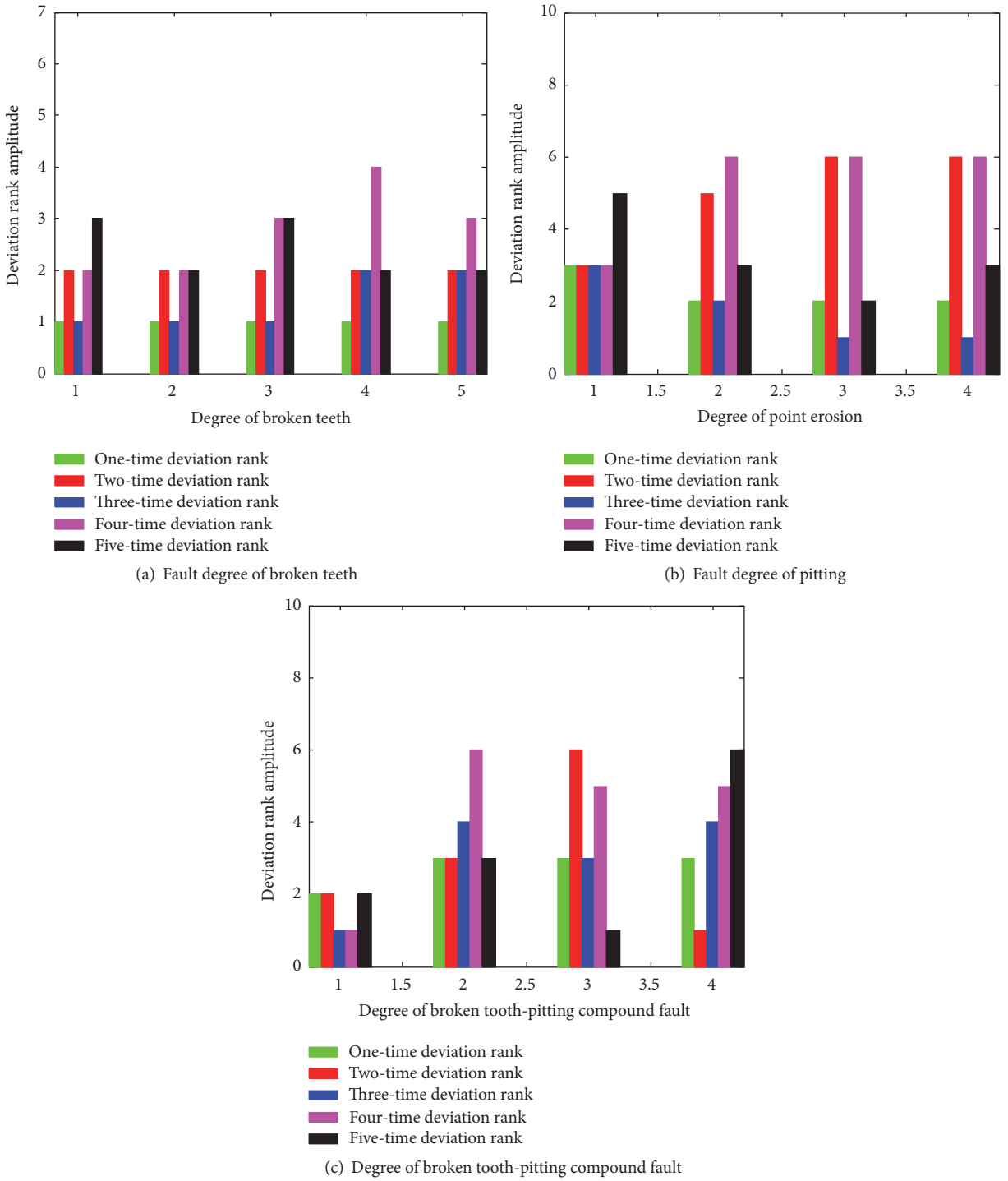

Figure 8: The relationship of absolute deviation rank between different fault degree and magnitude.

deviation within the range of 10 to 13 as grade IV, and setting the absolute deviation over 13 as grade V. Then Table 3 can be rewritten as Table 6.

The obtained consequences from simulation about different fault types of vibration frequency and amplitude absolute deviation level data are consistent with experimental data. It proved that this conclusion is correct. And it can accurately reflect the sensitive degree of fault type and provide quick reference to determine the fault degree for gear diagnosis.

6. Conclusion

In this paper, the different degree of broken teeth, pitting single fault, and broken teeth-pitting composite fault are

Table 4: The absolute deviation rank of different fault types vibration frequency amplitude.

Number	Fault type	Different fault of absolute deviation rank in mesh frequency and multiple frequency				
		$\lvert\Delta_1\rvert$	$\lvert\Delta_2\rvert$	$\lvert\Delta_3\rvert$	$\lvert\Delta_4\rvert$	$\lvert\Delta_5\rvert$
1	Normal model	0	0	0	0	0
2	1/5 broken teeth	0	I	0	I	II
3	2/5 broken teeth	0	I	0	I	I
4	3/5 broken teeth	0	I	0	II	II
5	4/5 broken teeth	0	I	I	III	I
6	Total broken teeth	0	I	I	II	I
7	Point erosion 1	II	II	II	II	IV
8	Point erosion 2	I	IV	I	V	II
9	Point erosion 3	I	V	0	V	I
10	Point erosion 4	I	V	0	V	II
11	Compound fault 1	I	I	0	0	I
12	Compound fault 2	II	II	III	V	II
13	Compound fault 3	II	V	II	IV	0
14	Compound fault 4	II	0	III	IV	V

Table 5: The fault experimental data.

Number	Fault type	Different fault of vibration amplitude in mesh frequency and multiple frequency				
		290 Hz	580 Hz	870 Hz	1160 Hz	1450 Hz
1	Normal model	2231	4127	2713	1073	2286
2	1/5 broken teeth	2236	4239	2732	1113	2383
3	2/5 broken teeth	2243	4200	2729	1094	2345
4	3/5 broken teeth	2246	4190	2725	1126	2397
5	4/5 broken teeth	2249	4215	2785	1157	2365
6	Total broken teeth	2251	4268	2809	1125	2341
7	Point erosion 1	2360	4341	2841	1145	2558
8	Point erosion 2	2291	4672	2756	1279	2437
9	Point erosion 3	2309	4684	2719	1246	2351
10	Point erosion 4	2322	4734	2726	1224	2392
11	Compound fault 1	2266	4284	2738	1079	2318
12	Compound fault 2	2335	4325	2974	1260	2430
13	Compound fault 3	2368	4695	2835	1208	2304
14	Compound fault 4	2379	4160	2936	1219	2593

Table 6: The level of absolute deviation of different fault types vibration frequency amplitude.

Number	Fault type	Different fault of absolute deviation rank in mesh frequency and multiple frequency				
		$\lvert\Delta_1\rvert$	$\lvert\Delta_2\rvert$	$\lvert\Delta_3\rvert$	$\lvert\Delta_4\rvert$	$\lvert\Delta_5\rvert$
1	Normal model	0	0	0	0	0
2	1/5 broken teeth	0	I	0	I	II
3	2/5 broken teeth	0	I	0	I	I
4	3/5 broken teeth	0	I	0	II	II
5	4/5 broken teeth	0	I	I	III	I
6	Total broken teeth	0	I	I	II	I
7	Point erosion 1	II	II	II	II	IV
8	Point erosion 2	I	IV	I	V	II
9	Point erosion 3	I	V	0	V	I
10	Point erosion 4	I	V	0	V	II
11	Compound fault 1	I	I	0	0	I
12	Compound fault 2	II	II	III	V	II
13	Compound fault 3	II	V	II	IV	0
14	Compound fault 4	II	0	III	IV	V

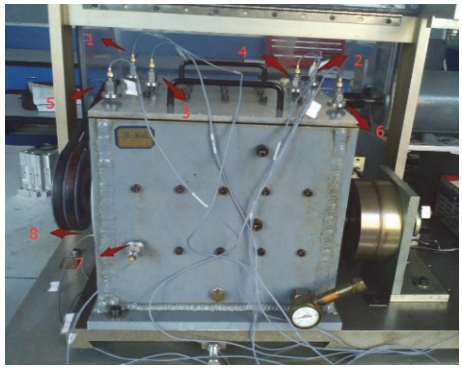

Figure 9: Sensor arrangement.

taken as research project. The results show that the method can get different degrees and different types of faults in the frequency doubling of meshing frequency by using the absolute deviation rank diagnostic approach for the gear broken teeth-pitting composite fault, and it is proved to be the most sensitive feature. According to the analysis of the corresponding characteristic frequency amplitude in the table to judge whether there is a fault in the gear, on the basis of the conclusion, the characteristics of the fault signal can achieve the purpose of identification about the different degree of broken teeth-pitting compound fault to broken teeth and pitting single fault.

Competing Interests

There is no conflict of interests regarding the publication of this paper.

Acknowledgments

Financial support from National Natural Science Foundation of China (51575178, 51175170, and 51375162) and financial support from China Scholarship Fund (201408430118) are appreciated.

References

[1] W. J. Staszewski, K. Worden, and G. R. Tomlinson, "Time–frequency analysis in gearbox fault detection using the Wigner–Ville distribution and pattern recognition," *Mechanical Systems and Signal Processing*, vol. 11, no. 5, pp. 673–692, 1997.

[2] H. Li, Y. Zhang, and H. Zheng, "Application of Hermitian wavelet to crack fault detection in gearbox," *Mechanical Systems and Signal Processing*, vol. 25, no. 4, pp. 1353–1363, 2011.

[3] G. Bin, X. Li, J. Wu, and J. Gao, "Virtual dynamic balancing method without trial weights for multi-rotor series shafting based on finite element model analysis," *Journal of Renewable and Sustainable Energy*, vol. 6, no. 4, Article ID 042014, 2014.

[4] P. N. Saavedra and C. G. Rodriguez, "Accurate assessment of computed order tracking," *Shock and Vibration*, vol. 13, no. 1, pp. 13–32, 2006.

[5] C. Kar and A. R. Mohanty, "Vibration and current transient monitoring for gearbox fault detection using multiresolution Fourier transform," *Journal of Sound and Vibration*, vol. 311, no. 1-2, pp. 109–132, 2008.

[6] Y. Lei and W. Tang, "ASTFA-BSS method and its application in the composite gearbox fault diagnosis," *Journal of Mechanical Engineering*, vol. 50, no. 17, pp. 61–68, 2014.

[7] X. Chen and D. Yu, "Gear box composite fault diagnosis method based on morphological component analysis and order tracking," *Journal of Aerospace Power*, vol. 29, no. 1, pp. 225–232, 2014.

[8] Y. Zhan, V. Makis, and A. K. S. Jardine, "Adaptive state detection of gearboxes under varying load conditions based on parametric modelling," *Mechanical Systems and Signal Processing*, vol. 20, no. 1, pp. 188–221, 2006.

[9] P. Velex and P. Sainsot, "An analytical study of tooth friction excitations in errorless spur and helical gears," *Mechanism and Machine Theory*, vol. 37, no. 7, pp. 641–658, 2002.

[10] F. Chaari, T. Fakhfakh, and M. Haddar, "Analytical modelling of spur gear tooth crack and influence on gearmesh stiffness, vol. 28, no. 3, pp. 461–468, 2009.

[11] A. Saxena, B. Wu, and G. Vachtsevanos, "A methodology for analyzing vibration data from planetary gear systems using complex morlet wavelets," in *Proceedings of the American Control Conference (ACC '05)*, pp. 4730–4735, Portland, Ore, USA, June 2005.

[12] S. Wang, M. Huo, C. Zhang et al., "Effect of mesh phase on wave vibration of spur planetary ring gear," *European Journal of Mechanics - A/Solids*, vol. 30, no. 6, pp. 820–827, 2011.

[13] W. Kim, J. Y. Lee, and J. Chung, "Dynamic analysis for a planetary gear with time-varying pressure angles and contact ratios," *Journal of Sound and Vibration*, vol. 331, no. 4, pp. 883–901, 2012.

[14] G. Bin, Z. Jiang, X. Li, and B. S. Dhillon, "Weighted multi-sensor data level fusion method of vibration signal based on correlation function," *Chinese Journal of Mechanical Engineering*, vol. 24, no. 5, pp. 899–904, 2011.

[15] Z. Fang, G. Shu, K. He et al., "Muti -body contact dynamic modeling of gear tran-smission," *Journal of Mechanical Transmission*, vol. 33, no. 1, pp. 15–19, 2009.

[16] L. Cui, C. Kang, L. Gao, F. Zhang, and S. Su, "Research on the vibration response and dynamic model a spur gear system with fault," *Journal of Vibration and Shock*, vol. 33, no. 1, pp. 15–19, 2009.

[17] D. R. Salgado and J. M. Del Castillo, "A method for detecting degenerate structures in planetary gear trains," *Mechanism and Machine Theory*, vol. 40, no. 8, pp. 948–962, 2005.